C.P. No. 491
(19,912)
A.R.C. Technical Report

C.P. No. 491
(19,912)
A.R.C. Technical Report

MINISTRY OF AVIATION

AERONAUTICAL RESEARCH COUNCIL

CURRENT PAPERS

A Wind Tunnel Investigation into the Factors Affecting the Spanwise Load Distribution over the Vertical Tail Surface of an Aircraft having a Wedge-Type Rear Fuselage

by

K. F. S. Chard and J. Deakin

With a Foreword and an Appendix

by

A. R. Collar

LONDON: HER MAJESTY'S STATIONERY OFFICE

1960

Price 4s 6d net

C.P. No.491

A Wind Tunnel Investigation into the Factors affecting the Spanwise Load Distribution over the Vertical Tail Surface of an Aircraft having a Wedge-Type Rear Fuselage

- By -
K. F. S. Chard and J. Deakin

With a Foreword and an Appendix
- By -
A. R. Collar

Report No.31
Department of Aeronautical Engineering,
University of Bristol

18th February, 1958

FOREWORD

This report, in its original form, was submitted by the authors as part of the requirement for the Degree of B.Sc. in Engineering with Honours of the University of Bristol. However, descriptive material that is quite appropriate in a thesis or dissertation can be out of place in a scientific communication; the present writer has therefore severely edited the original for its present purpose. The editing has taken the form, mainly, of deletion of sections judged inappropriate; if therefore in its present form the report lacks something in continuity, the writer must accept responsibility.

There are two points on which comment must be offered. First, it is perhaps not entirely clear that the vortex system shown in Fig. 13 represents the additional vorticity due to the introduction of the fin (and rudder), compared with the condition with fin absent: so far as the fin is concerned, the additional vorticity is, of course, also the total vorticity. Any induced velocities due to initial vorticity in the remaining surfaces are assumed to be included in the measurements of velocity and direction with fin absent.

The second point concerns the discrepancy between the measured load and that predicted from the vortex system of Fig. 13 and Appendix I. The authors suggest in § 6 that this may be due to curvature of flow. However, the present writer has demonstrated that about half the discrepancy can be attributed to the use of a finite number of horseshoe vortices to represent the continuous distribution: the results of this investigation are summarised in Appendix II.

SUMMARY/

SUMMARY

A wind tunnel model of a typical low-speed, straight-winged aircraft, having a wedge-type rear fuselage, was designed for an investigation of the factors affecting the spanwise load distribution over the vertical tail with the aircraft in a yawed attitude. The model incorporated two alternate wing positions, three wing aspect ratios, three different cockpits, three tailplane positions and a movable rudder; but the tests described here are limited to two tailplane positions. A propeller was not fitted. The fin and rudder surfaces were fitted with orifices for pressure distribution tests.

An approximate method is proposed for predicting the spanwise load distribution over the vertical tail in yaw, from a knowledge of the variation of direction and velocity of the airflow in the region of the vertical tail with this surface removed.

The tests were made with the low mounted wings at an aspect ratio of 7, and with a large unfaired cockpit, at a Reynolds number of 0.2×10^6 (based on the mean chord of the vertical tail of aspect ratio 1.0) with the tailplane at high and low positions on the rear fuselage. The tests revealed considerable variation in the direction of flow in the region of the vertical tail. This variation of flow direction had an appreciable effect on the spanwise load distribution over the vertical tail. Pressure distribution tests showed a low value of spanwise load near the base of the vertical tail and a maximum value at three quarters span.

The proposed method of predicting the vertical tail spanwise load distribution gave load values 25% higher than the values determined from the pressure distribution tests, but is promising in that the predicted distribution was similar in form to the measured distribution.

CONTENTS

5./

---

1. Introduction

The distribution of the air loads on the vertical tail surface or surfaces of an aircraft during flight must be accurately estimated during design of the aircraft to satisfy stressing and stability requirements. Several methods of calculating the spanwise load distribution on unswept wings at low speeds are in use, but their application to the vertical tail surfaces gives rise to inaccurate results, owing to the complicated nature of the airflow in the region of the rear fuselage. It is not unusual for the design of the vertical tail surfaces to be changed during initial wind tunnel tests so that stability criteria should be satisfied, but the most efficient stressing has not always been possible due to uncertainties during design concerning the air load distribution.

Methods of calculating a realistic approximation to the chordwise load distribution on unswept tail surfaces at low speeds are available[1], while several reports concerning stability characteristics, pressure distributions and other features of such tail units have been published, two of the most important being those by Pass[2] and by Lyons and Bisgood[3]. The latter gives a design method for vertical tails which includes a theoretical spanwise lift distribution. Marino and Mastracola[4] have drawn attention to departures from the expected distribution. These writers also criticise the definition of vertical tail surface area used by Pass[2] in his analysis of several different aircraft. Several reports have described an analysis of the airflow in the region of the vertical tail with this surface removed, and it is clear that this flow is not uniform. Other reports on the subject are not compatible due to differing assumptions and test conditions. To the knowledge of the writers, the effect of cockpit size or configuration on the airflow around the vertical tail has not been investigated.

The apparatus described below was designed for an investigation into the spanwise air load distribution over the single vertical tail surface of a model aircraft having a wedge-type rear fuselage, i.e., the rear fuselage terminates in a vertical sternpost which carries part of the rudder hinge, so that the rudder extends over the full depth of the fuselage. The model could be assembled in several different configurations, so that the effects of different features on the spanwise load distribution on the vertical tail could be studied.

The/

The end-plate effect of the tailplane could be investigated by tests with the tailplane in high, mid or low positions on the rear fuselage, and three different cockpits were available for comparative purposes. Effects due to low or shoulder wing position, to variation of wing aspect ratio, and to rudder deflection could also be studied. It was originally intended to have several vertical tails of different aspect ratios, but shortage of time precluded the construction of more than one. As no propeller was fitted, the effects of slipstream rotation could not be investigated.

An Appendix to this report describes an approximate method for calculating the spanwise load distribution which takes into account the variation in velocity and direction of the airflow on the vertical tail quarter chord line in the absence of the vertical tail, as well as effects due to variation of vertical tail aspect ratio and the induced effects due to the horizontal tail. The writers are unaware of any previous theory which includes consideration of all these factors in the prediction of vertical tail spanwise load distribution.

2. Description of Apparatus

2.1 Model

The model shown in Fig. 1*, was designed to be representative of small low-speed aircraft. A large number of configurations could be obtained by varying the position of its components so that most of the parameters affecting tail loading could be investigated on a single model. It was desirable to make the model as large as possible so that a system of pressure transmission tubes could be built into the fin and passed through the rear fuselage without undue complexity or congestion, but the model size was restricted, by the necessity of avoiding excessive wind tunnel boundary constraint effects, to a maximum span of 36 inches. The model was made of laminated mahogany, with the exception of the perspex fin and moulded resin rudder. Ebony was used for the wing and tailplane trailing edge and all metal fittings were of brass.

2.1.1 Wings

The wings, which were of RAF 38 aerofoil section and had 3° dihedral, could be fitted into the fuselage at zero angle of attack in low or shoulder position. Detachable wing tips were fitted so that aspect ratios of 9, 7 and 5 were available.

2.1.2 Fuselage

The fuselage was of rectangular section with rounded corners. In addition to cut-outs for the two wing positions and tail unit, the top decking was cut away so that three different cockpits, representing large and small unfaired and small faired types, could be fitted. The rear fuselage, shown in detail in Fig. 6, had three horizontal slots cut in it to mount the tailplane in high, mid or low positions, and a vertical slot for the fin or fin blank. Channels cut in the rear fuselage for the pressure transmission tubes from the fin led to a common outlet, fitted with a short aerofoil section tube, under the rear fuselage.

2.1.3 Tail unit

The NACA 0010 aerofoil section was used for the tailplane which had a "cut out" at the trailing edge to allow for rudder movement. A brass centre section was used for strength reasons, and brass fittings were used at the tips to retain the tail suspension

wires/

---

*Figs. 3, 4, 5 of this report are not reproduced here.

wires of the mounting system. The tailplane and tailplane blanks fitted in the unused tailplane slots were held in place by the fin or fin blank, these being retained by two bolts through the fuselage. The fin blank could be fitted in the rear fuselage in place of the base of the fin for tests with the fin removed, and carried a brass extension used for supporting the rear of the model in tests with the tailplane removed.

The vertical tail surface of NACA 0010 section and aspect ratio 1.0 is shown in Fig. 6. Several spanwise brass tubes were placed at various chordwise positions flush with the surface of the perspex fin. Each tube had 0.06 inch diameter holes drilled into it at regular spanwise intervals and was led through the base of the fin into the fuselage. Flexible plastic pressure transmission tubes from the base of the rudder were passed into the fuselage through a channel in the base of the fin. The vertical rudder hinge line was at 60% chord, the rudder being made of "Crystic 189" polyester resin moulded around five spanwise brass pressure transmission tubes which had 0.06 inch diameter holes drilled into them at regular spanwise intervals. A series of brass plates of aerofoil section, each with the part above the rudder at a different angle to the fin centre line, was made. These could be screwed to the tip of the fin so that the rudder could be held in a series of deflected positions.

2.2 Mounting system

The model was mounted in the working section of a 4 foot diameter open section closed circuit wind tunnel by a system of suspension wires, shown in Fig. 2. An angular movement in yaw of $\pm 20^{\circ}$ was available. Weights hanging from the model suspension points were immersed in oil to reduce vibration of the model, which was mounted inverted.

2.3 Measuring apparatus

The angle of yaw of the model was measured by a rotatable hairline telescope fitted with a pointer. This was mounted, together with a fixed protractor scale, on the wind tunnel balance above the baseboard, and viewed the model through a tube in the centre of the turntable (Fig. 2).

A multitube manometer was used to measure the pressures transmitted from the fin and rudder. The airflow characteristics around the tail of the model were found by using small pitot and static pressure heads and a twin bevelled tube (Conrad) yawmeter head. Small diameter plastic tubes from the pressure heads transmitted pitot or static pressure to a Chattock gauge.

3. Method

3.1 Development of apparatus

As several holes were drilled into each fin and rudder pressure tube, it was necessary to cover all those except the ones at the chordwise station where pressure readings were required. Narrow strips of thin gauge transparent adhesive tape were found to form a successful seal provided care was taken in application, and nail varnish was used to seal holes where the surface curvature prevented successful application of the adhesive tape.

3.2/

3.2 Test procedure

The model was assembled with the wings of aspect ratio 7 in the low position and the large unfaired cockpit in place. The only vertical tail available for the tests had an aspect ratio of 1.0, this being at the lower end of the proposed range of vertical tail aspect ratios. This model configuration was used for a series of tests with the tailplane fitted in both the low and high positions.

To allow for displacement of the model due to air loads, the desired incidence and yaw were set up with the tunnel running at the test airspeed of 116 feet per second (a Reynolds number of 0.2×10^6 based on vertical tail mean chord).

For the first tests the fin was removed and replaced by the fin blank. The cantilever beam traversing equipment was set up in position with the yawmeter head placed at a point on the vertical tail quarter chord line near the root position, due allowance being made for the movement of the model and beam under air loads. A quarter chord line traverse of the vertical tail was then made to determine the angles of sidewash over the fin by obtaining null readings on the U-tube connected to the yawmeter. Similar traverses were then made with the pitot and static pressure heads, the sidewash readings being used to ensure that the pressure heads pointed directly into the airstream.

The fin was then fitted and multitube manometer pressure records obtained in the usual way.

The above tests were made with the model at 0° incidence and 8° yaw for the tailplane in both high and low positions.

4. Presentation of Results

The results of the vertical tail quarter chord line traverses with low and high tailplane positions are shown graphically in Figs. 7 and 8 respectively, variation of measured incidence on the vertical tail being plotted in radians and the dynamic head and velocity variations plotted non-dimensionally in terms of the free stream value of dynamic head and velocity. The velocity variation is derived from the dynamic head variation.

Chordwise pressure distributions at each reference section are plotted, in terms of pressure coefficients based on free stream dynamic pressure, in Figs. 9 and 10. The area under the curves is integrated for the normal force coefficient at each section. This coefficient is then multiplied by the local chord and free stream dynamic pressure to give the lift per unit span at each section, as shown in Figs. 11 and 12 for the low tailplane and high tailplane cases respectively. These figures also show the spanwise lift distribution predicted by the method of Appendix I from the quarter chord line traverse.

5. Discussion of Results

5.1 Vertical tail quarter chord line traverse

Figs. 7a and 8a show that the variation of the total angle of incidence of the airflow on to the vertical tail is considerable. Near the base of the vertical tail the flow tends to be parallel to the centreline of the aircraft or even to have greater yaw; but at about one eighth span the direction changes sharply, flowing across the fuselage and at 0.25 to 0.3 radian to the centreline: this nearly doubles the fin incidence due to yaw alone. The angle of flow

relative/

relative to the fuselage thereafter decreases and tends towards the free stream direction, but does not attain this direction within the span.

Figs. 7b, 7c, 8b and 8c indicate that the values of the dynamic head and velocity of the airflow in the vicinity of the base of the fin are about 35% and 20% respectively below the free stream values. This effect extends beyond the estimated thickness of the fuselage boundary layer and may possibly be due to the presence of a turbulent wake from the cockpit or the wing fuselage intersection. The free stream values of dynamic head and velocity are reached at about 80% vertical tail span.

5.2 Vertical tail chordwise pressure distribution

The chordwise pressure coefficient variation (Figs. 9 and 10) is of normal form except at the base of the vertical tail where negative pressures occur near the leading edge on the positive pressure side of the surface. This is presumably due to the negative angle of incidence of the flow on to the surface at this point. The maximum stagnation pressure coefficients at sections D, E and F are seen to be less than unity. This is because the pressure coefficients are based upon the free stream dynamic pressure, whereas the dynamic pressure in the vicinity of these sections is less than the free stream value (Figs. 7b and 8b).

5.3 Vertical tail spanwise load distribution (Figs. 11 and 12)

The spanwise load distribution obtained for both tailplane positions is similar in general form to the distributions obtained by Marino and Mastrocola[4]. The maximum value occurs at about 55% span and drops rapidly to a low value near the base of the vertical tail. The curves of measured lift per unit span are similar in form for both low and high tailplane cases, the maximum value for the low tailplane case being 10% higher than that for the high tailplane case. This is probably due to the greater effective aspect ratio of the vertical tail resulting from the lower tailplane position, as shown by Riley[5]. The variation of vertical tail loading due to tailplane vertical and fore and aft location is a suitable subject for further investigation with this model.

The curves of predicted spanwise load distribution are seen to be of very similar form to the curves of measured distribution, although the predicted values are approximately 25% greater in both low and high tailplane cases. The fact that the corresponding values of the predicted and measured distribution curves are in very nearly constant ratio over the complete span provides some measure of verification of the prediction. It is possible that the 25% discrepancy was due to curvature of the flow in the region of the vertical tail producing an effective curvature of this surface.* This possible curvature of the flow could be investigated by making yawmeter traverses on the leading and trailing edge lines with the vertical tail removed. Thus any effective camber could be determined and incorporated in the spanwise loading prediction.

A noticeable feature of the load distribution curves is a small kink which occurs in both the predicted and measured curves at about 75% span, for both the high and low tailplane cases. The fact that the kink appears in all four curves suggests that it is not due to experimental errors, and it is noticed that there is a slight variation in sidewash and dynamic head at 75% span for the quarter chord

line/

*See also Appendix II.

line traverse results (Figs. 7 and 8). This slight variation probably causes the kink in the predicted curve as this is derived from relationships incorporating the airflow characteristics. The reason for the local variation in the distribution curves is unknown but it is suggested that, considering its spanwise position, it may be due to the effects of a vortex shed from the large unfaired cockpit. Further tests with the three different cockpits are necessary to check this suggestion.

6. Conclusions

The variation of sidewash in the region of the vertical tail is large and has a major effect on the spanwise load distribution of the vertical tail. The dynamic head and velocity of the airflow in the region of the base of the vertical tail are below free stream values, and this effect extends well beyond the thickness of the estimated fuselage boundary layer. It may be due to the presence of a turbulent wake from the cockpit or wing root.

The method of Appendix I accurately predicts the form of the vertical tail spanwise load distribution and in this respect is promising. However, the predicted values are approximately 25% higher than the measured values of load per unit span. Further work investigating the curvature of the airflow in the region of the vertical tail and the pressure distribution over the sides of the rear fuselage may reduce this discrepancy between measured and predicted load distributions. The proposed method of predicting the vertical tail spanwise load distribution shows sufficient promise to justify continuation of this investigation.

Further experimental work should be carried out with the existing model in order to develop a reliable empirical or theoretical method of predicting the airflow characteristics in the region of the vertical tail. The method should incorporate the effects of variations in the aircraft configuration (viz., aspect ratio, wing position, cabin shape, tailplane position and rudder deflection), aircraft attitude (angles of incidence and yaw) and eventually, after the addition of a propeller or propellers to a similar model, slipstream rotation.

If such a method were successful, the theory developed in Appendix I would then lead to a method of estimating a reasonable approximation to the spanwise load distribution over the vertical tail surface of conventional low-speed straight winged aircraft having a wedge-type rear fuselage.

References/

References

No.	Author(s)	Title, etc.
1		Joint Airworthiness Committee. Paper No.576, September, 1952.
2	H. R. Pass	Analysis of wind-tunnel data on directional stability and control. N.A.C.A. Technical Note No.775, September, 1940. A.R.C. 4762 28th October, 1940.
3	D. J. Lyons and P. L. Bisgood	An analysis of the lift slope of aerofoils of small aspect ratio, including fins, with design charts for aerofoils and control surfaces. A.R.C. R.& M. 2308. January, 1945.
4	Alfred A. Marino and N. Mastrocola	Wind-tunnel investigation of the contribution of a vertical tail to the directional stability of a fighter-type airplane. N.A.C.A. Technical Note No.2488, January, 1952.
5	Donald R. Riley	Effect of horizontal-tail span and vertical location on the aerodynamic characteristics of an unswept tail assembly in sideslip. N.A.C.A. Technical Note No.2907, February, 1953.
6	A. R. Collar	On the accuracy of the representation of a lifting line by a finite set of horseshoe vortices A.R.C. 19,764 December, 1957.

Acknowledgement

The writers wish to acknowledge the assistance of Mr. R. P. Boswell.

APPENDIX I/

APPENDIX I

The Approximate Estimation of Spanwise Load Distribution on the Vertical Tail in a Yawed Condition using Measurements of Airflow Characteristics with the Vertical Tail Removed

---

A.1.1 Introduction

The load distribution on the vertical tail in yaw depends on the variation of dynamic pressure and sidewash due to the aircraft as a whole, on the induced effects of the horizontal tail and the rear section of the fuselage and on its own induced effects. If the vertical tail is removed and yaw and dynamic pressure traverses are made on the quarter chord line of the vertical tail the following effects will be measured: the variation of dynamic pressure and sidewash due to the aircraft as a whole, the induced effect of the rear fuselage and that part of the induced effect of the horizontal tail which arises through interaction with the rear fuselage.

When the vertical tail is replaced its induced effects will increase the rear fuselage load. The following analysis is based on measurements of flow direction and velocity made with the vertical tail removed; it incorporates the induced effects which occur when the vertical tail is replaced.

A.1.2 Outline of Method

The tail surfaces are represented by a set of finite horseshoe vortices, the bound part of each vortex lying on the quarter chord line of the surface it represents (Fig. 13). The contribution of the fuselage is also represented by horseshoe vortices lying on the projection of the vertical tail quarter chord line.

The induced incidence at the centre of the bound portion of each vortex, due to all the other vortices, is calculated. In the case of the vertical tail the angle of yaw and values of the sidewash on the quarter chord line, measured with the vertical tail removed, are added to the induced incidence. Measured variation of the dynamic pressure on the quarter chord line of the vertical tail is also incorporated. This leads to a number of simultaneous linear equations, equal to the number of horseshoe vortices, for the normal force per unit span at each section.

A.1.3 Symbols

K	Strength of a horseshoe vortex
v	induced sidewash velocity at a point on the vertical tail
w	induced downwash velocity at a point on the horizontal tail
L	normal force per unit span
q	dynamic pressure
V	local wind velocity
c	local chord

α effective incidence angle, including induced angle (radians)

γ measured incidence angle (radians)

a_v, a_h two-dimensional slope of the lift coefficient, incidence curve of the vertical and horizontal tail surfaces

ρ air density

$y, z, a_1, a_2, b_1, b_2, c_1, c_2, s_1, s_2$ dimensions indicated in Fig. 15.

The positive sense of all quantities is indicated in Figs. 14 and 15.

A.1.4 Suffices

h Of the horizontal tail

v of the vertical tail

y at point B indicated in Fig. 15

z at point A indicated in Fig. 15

o free stream

r due to a vortex of the horizontal tail

s due to a vortex of the vertical tail.

A.1.5 Assumptions

The following assumptions have been made.-

(i) The quarter chord lines of the vertical and horizontal tail surfaces are straight and coincident.

(ii) The conditions affecting the horizontal tail, when the vertical tail is removed, are the free stream conditions.

(iii) No part of the tail surfaces is stalled.

(iv) The effect of a constant incidence on the horizontal tail is to produce a flow pattern which is symmetrical about the vertical plane through the centre line of the aircraft and which does not, therefore, produce a load on the vertical tail.

(v) The trailing sections of the horseshoe vortices are parallel to the centre line of the aircraft. (This assumption implies that the loading of the horizontal tail induced by the vertical tail is antisymmetric.)

A.1.6/

A.1.6 Derivation of Equations (Figs. 14 and 15)

Sidewash velocity at A, due to horseshoe vortex K_m is

$$v_r = \frac{K_m}{4\pi}.z\left[\frac{1}{z^2 + a_2^2} - \frac{1}{z^2 + a_1^2}\right].$$

Downwash velocity at B due to horseshoe vortex K_m is

$$w_r = \frac{K_m}{4\pi}\left[\frac{1}{b_2} - \frac{1}{b_1}\right].$$

Sidewash velocity at A due to horseshoe vortex K_n is

$$v_s = \frac{K_n}{4\pi}\left[\frac{1}{a_2} - \frac{1}{d_1}\right].$$

Downwash velocity at B due to horseshoe vortex K_n is

$$w_s = \frac{K_n}{4\pi}.y\left[\frac{1}{y^2 + c_2^2} - \frac{1}{y^2 + c_1^2}\right].$$

Now $L_m = \rho V_o K_m$ and $L_n = \rho V_n K_n$, per unit span.

Therefore $K_m = \frac{L_m}{\rho V_o}$ and $K_n = \frac{L_n}{\rho V_n}$.

Therefore, summing the sidewash velocities at point A due to all the vortices

$$v_z = \sum \frac{L_m}{4\pi}.z\left[\frac{1}{z^2 + a_2^2} - \frac{1}{z^2 + a_1^2}\right] + \sum \frac{L_n}{4\pi}\left[\frac{1}{d_2} - \frac{1}{d_1}\right]$$

$$= \sum \frac{L_m}{4\pi\rho V_o}.z\left[\frac{1}{z^2 + c_2^2} - \frac{1}{z^2 + a_1^2}\right] + \sum \frac{L_n}{4\pi\rho V_n}\left[\frac{1}{d_2} - \frac{1}{d_1}\right].$$

For the vertical tail

$$L_z = \tfrac{1}{2}\rho V_z^2 c_z a_v \theta_z$$

and

$$\theta_z = \gamma_z - \frac{v_z}{V_z}$$

therefore

$$\frac{2L_z}{\rho V_z^2 c_z a_v} - \gamma_z = -\frac{v_z}{V_z}$$

$$= \sum \frac{L_m}{4\pi\rho V_o V_z} z\left[\frac{1}{z^2 + a_1^2} - \frac{1}{z^2 + a_2^2}\right] + \sum \frac{L_n}{4\pi\rho V_n V_z}\left[\frac{1}{d_1} - \frac{1}{d_2}\right].$$

Multiply/

Multiply by $\frac{1}{2}\rho V_o^2 \left(\frac{V_z}{V_o}\right)$, put $\frac{1}{2}\rho V_o^2 = q_o$ and rearrange

$$8\pi \left[\frac{L_z}{(V_z/V_o)c_z a_v} - q_o y_z \left(\frac{V_z}{V_o}\right) \right] = \sum L_m . z \left[\frac{1}{z^2 + a_1^2} - \frac{1}{z^2 + a_2^2} \right]$$

$$+ \sum \frac{L_n}{(V_n/V_o)} \left[\frac{1}{d_1} - \frac{1}{d_2} \right]. \qquad \ldots(1)$$

Similarly for the horizontal tail

$$\frac{8\pi L_y}{c_y a_h} = \sum L_m \left[\frac{1}{b_1} - \frac{1}{b_2} \right] + \sum \frac{L_n}{(V_n/V_o)} . y \left[\frac{1}{y^2 + c_1^2} - \frac{1}{y^2 + c_2^2} \right].$$

$\ldots(2)$

The number of equations for the horizontal tail may be halved by using the fact that the loading is antisymmetrical.

A.1.7 The Effective Chord and Lift Slope of the Fuselage

There are two indeterminate quantities involved in the above analysis; the effective chord and lift slope of the fuselage, which appear in the equations as a product. The value of the chord was taken arbitrarily as the root chord of the vertical tail.

Side loads act on a yawed fuselage when the vertical tail is removed and the corresponding induced flow affects the measured value of the sidewash on the quarter chord line. When the fin is replaced its induced effects cause an increase in the fuselage load. It is this increase in fuselage load which must be incorporated in the equations, because only this part of the fuselage load produces further induced flow on the vertical tail. A value of 1.5 was arbitrarily chosen as being a reasonable value for the effective lift slope of the fuselage, in conjunction with the chosen value of the effective chord. This value was justified only by comparison of the form of the predicted fin load distribution with the actual distribution. Further work, determining this value for various forms of rear fuselage would be useful, but it should be noted that errors in this value only produce small errors in the fin loading.

A.1.8 Application to the Wind Tunnel Model

The fuselage and vertical tail were represented by eleven equi-span horseshoe vortices, numbers one to five representing the fuselage and numbers six to eleven representing the vertical tail. This number was chosen because the centre lines of the low and high horizontal tail positions and the base of the fin fitted almost exactly between the vortices. The horizontal tail was represented by six equi-span horseshoe vortices. Since the loading of the horizontal tail is antisymmetrical (see Appendix I, Section 5 (v)) there are only three unknowns and hence only three equations for the horizontal tail which are numbered twelve, thirteen and fourteen. The number of each horseshoe vortex may conveniently be used as a suffix for the quantities at the centre of its span. The values incorporated in the equations are presented in Tables 1 and 2.

Two/

Two typical examples of the fourteen simultaneous equations for the low horizontal tail case are shown below.

$$\frac{8\pi}{12}\left[\frac{12L_7}{0.85 \times 3.58 \times 5.97} - 16.03 \times 0.275 \times 0.85\right] + 8\,\frac{L_7}{0.85}$$

$$= 0.06L_1 + 0.08L_2 + 0.13L_3 + 0.23L_4 + 0.53L_5 + 2.67\,\frac{L_6}{0.84} + 2.67\,\frac{L_8}{0.93}$$

$$+ 0.53L_9 + 0.23L_{10} + 0.13L_{11} + 0.16L_{12} + 0.23L_{13} + 0.13L_{14}$$

$$\frac{8\pi L_{12}}{3.09 \times 5.97} + 3.56L_{12} = -0.41L_1 + 0.41L_2 + 0.44L_3 + 0.21L_4 + 0.10L_5$$

$$+ 0.05\,\frac{L_6}{0.84} + 0.03\,\frac{L_7}{0.85} + 0.02\,\frac{L_8}{0.93} + 0.01L_9 + 0.01L_{10} + 0.01L_{11}$$

$$+ 0.71L_{13} + 0.10L_{14}.$$

The equations were solved by an iterative method. Assumed values of L were inserted in each equation in turn leading to better approximate values of L which could then be substituted in the other equations.

It was found that the values could be made to converge within one half per cent after three or four iterations by making reasonably accurate initial assumptions.

APPENDIX II/

APPENDIX II

The Effect of a Finite Number of Horseshoe Vortices on Estimated Load

- By -
A. R. Collar

A.2.1 Introduction

In A.R.C. 19,784[6] the writer has compared the load due to a finite set of horseshoe vortices of equal span with the load due to the correct continuous distribution of vorticity. It is assumed that the downwash at the centre of each bound vortex equals the downwash at that point due to the continuous distribution, and that the circulation is determined wholly by the downwash.

For an elliptically loaded wing, it emerges that the ratio of the total load due to a set of m equally spaced horseshoe vortices to the true load is in these circumstances

$$R_m = \frac{m + 1}{m}; \qquad \ldots(A.2.1)$$

another example shows that the same result is approximately true when the loading is not elliptic.

A.2.2 Application to the Present Paper

Certain other factors are involved in the application of the above result to the investigations of the present paper. Here the circulation is determined partly by geometric incidence and partly by downwash. Consider an untwisted elliptic wing of aspect ratio A. As is well-known, the slope of the lift curve of such a wing bears a ratio to the two-dimensional slope of

$$\frac{A}{A + 2}.$$

This result derives from the fact that, if the geometric incidence is θ, it is the sum of two terms:

$$\text{induced incidence} = \frac{2}{A + 2}\,\theta$$

$$\text{effective incidence} = \frac{A}{A + 2}\,\theta.$$

Now from equation (A.2.1) we have that the excess load due to the use of m vortices is

$$R_m - 1 = \frac{1}{m},$$

expressed as a fraction of the true load. In the present instance, however, only the fraction $2/A+2$ of the total incidence is due to downwash; we may therefore expect the error to be reduced in this ratio

Hence/

Hence $$R_m - 1 = \frac{2}{m(A + 2)}. \qquad \ldots(A.2.2)$$

A.2.3 Check Calculations

To check the validity of equation (A.2.2), calculations have been made by methods identical to those of Appendix I for an untwisted elliptic wing, using six horseshoe vortices. The algebraic equations for the components of load were obtained with A general, and then solved for $A = 0, 1, 6, \infty$. The results agreed closely with equation (A.2.2) for $m = 6$. Indeed, exact agreement would presumably have resulted had it not been that it is necessary to assign arbitrarily, in some measure, the mean chords of the sections of the wing of finite span $s/3$, where $2s$ is the total span.

A.2.4 Application to the Results of Appendix I

In the calculations of Chard and Deakin for the tail unit of the present paper, the distribution of load is roughly elliptic (see Figs. 11, 12) and $m = 6$ over the tailplane span. Moreover, the aspect ratio A is unity. Accordingly, (A.2.2) gives

$$R_m = 1 + \frac{2}{6.3} = 1.11$$

and the estimated load may be expected to be 11% higher than the true load. In fact, the discrepancy is about twice this amount; presumably the remainder of the discrepancy must be due to curvilinearity of flow or other factors.

Tables/

Tables 1 and 2: Values Incorporated in Horseshoe Vortex Calculations

Table 1

Tailplane in Low Position

Vortex No.	1-5	6	7	8	9	10	11	12	13	14
y_z	0.14	-0.01	0.275	0.28	0.235	0.195	0.19	-	-	-
V_z/V_o	1.0	0.84	0.85	0.93	1.0	1.0	1.0	-	-	-
c_z inches	4.0	3.82	3.58	3.34	3.10	2.86	2.62	3.09	2.87	2.12
a	1.5	5.97	5.97	5.97	5.97	5.97	5.97	5.97	5.97	5.97

Table 2

Tailplane in High Position

Vortex No.	1-5	6	7	8	9	10	11	12	13	14
y_z	0.14	-0.04	0.21	0.26	0.23	0.195	0.19	-	-	-
V_z/V_o	1.0	0.89	0.82	0.82	1.0	1.0	1.0	-	-	-
c_z inches	4.0	3.82	3.58	3.34	3.10	2.86	2.62	3.09	2.87	2.12
a	1.5	5.97	5.97	5.97	5.97	5.97	5.97	5.97	5.97	5.97

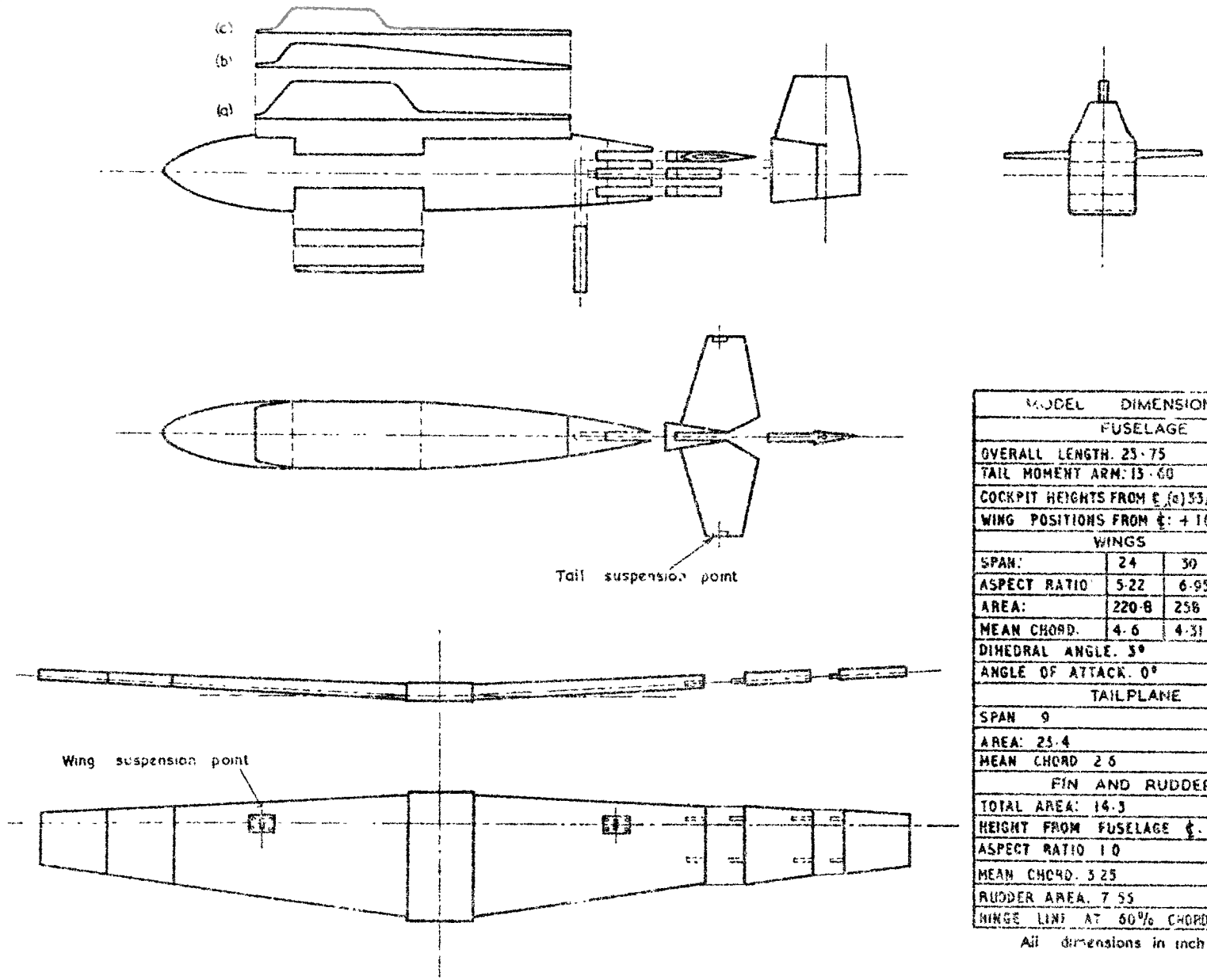

MODEL DIMENSIONS			
FUSELAGE			
OVERALL LENGTH. 25·75			
TAIL MOMENT ARM. 13·60			
COCKPIT HEIGHTS FROM ℄ (a) 3·3 (b) (c) 2·65			
WING POSITIONS FROM ℄: 4·10 - 1·3.			
WINGS			
SPAN:	24	30	36
ASPECT RATIO	5·22	6·95	8·04
AREA:	220·8	256·8	290·2
MEAN CHORD.	4·6	4·31	4·03
DIHEDRAL ANGLE. 3°			
ANGLE OF ATTACK. 0°			
TAILPLANE			
SPAN 9			
AREA: 23·4			
MEAN CHORD 2·6			
FIN AND RUDDER			
TOTAL AREA: 14·3			
HEIGHT FROM FUSELAGE ℄. 4·4			
ASPECT RATIO 1·0			
MEAN CHORD. 3·25			
RUDDER AREA. 7·55			
HINGE LINE AT 60% CHORD			

All dimensions in inch units

EXPLODED VIEWS OF MODEL, AND MODEL DIMENSIONS

FIG. 1

FIG. 2.

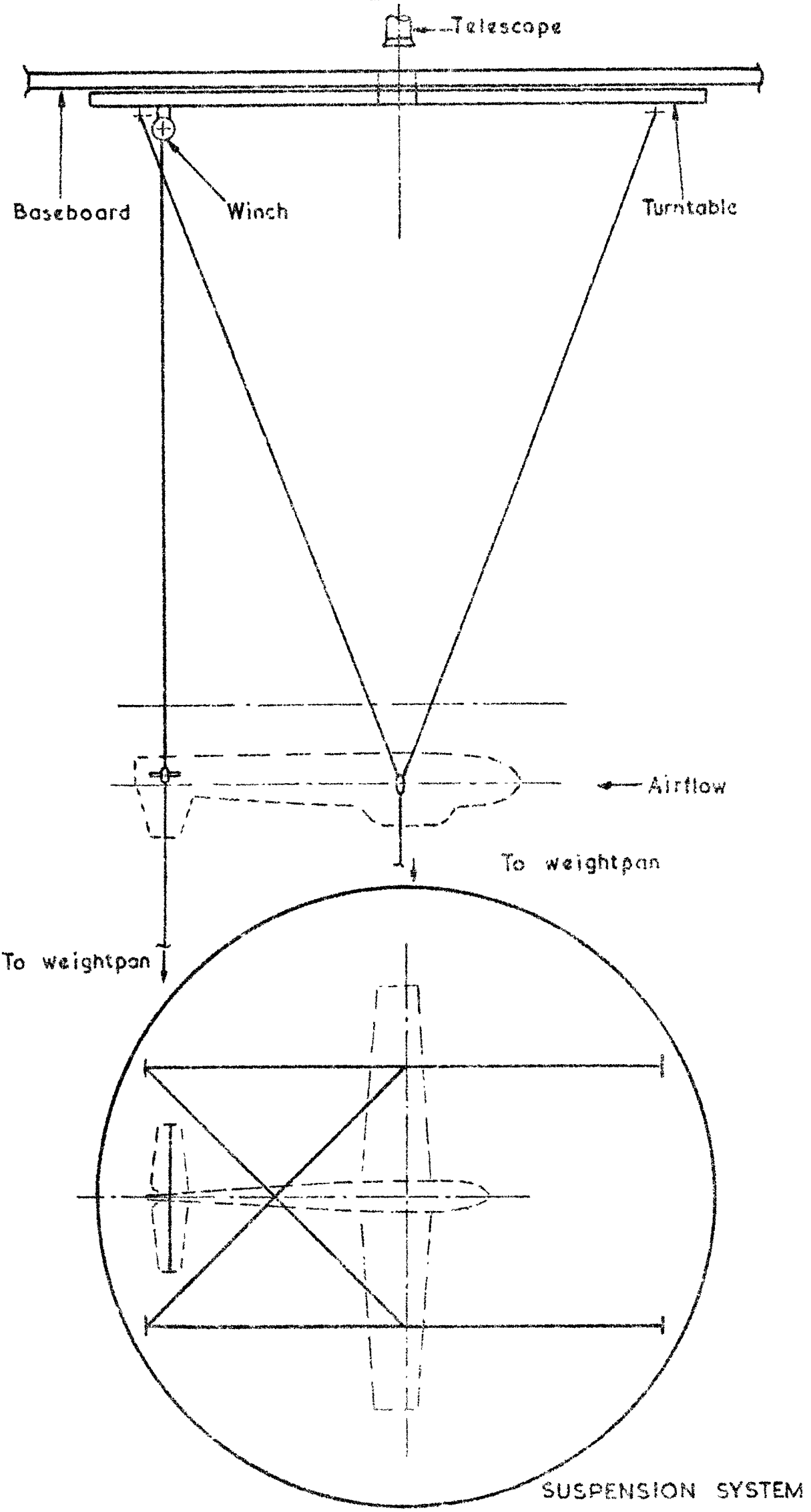

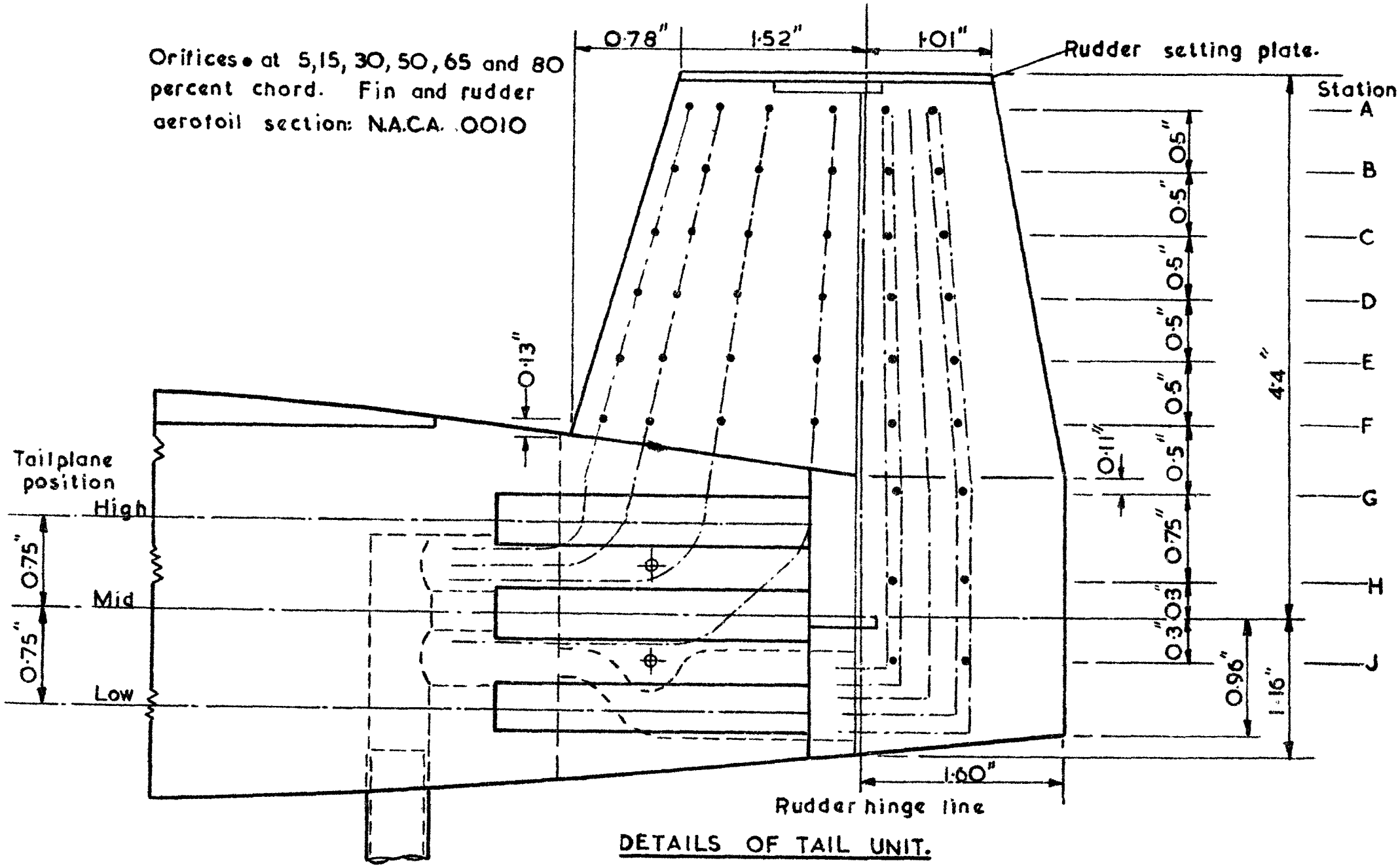

DETAILS OF TAIL UNIT.

FIG 9

FIG. 7.a-c.

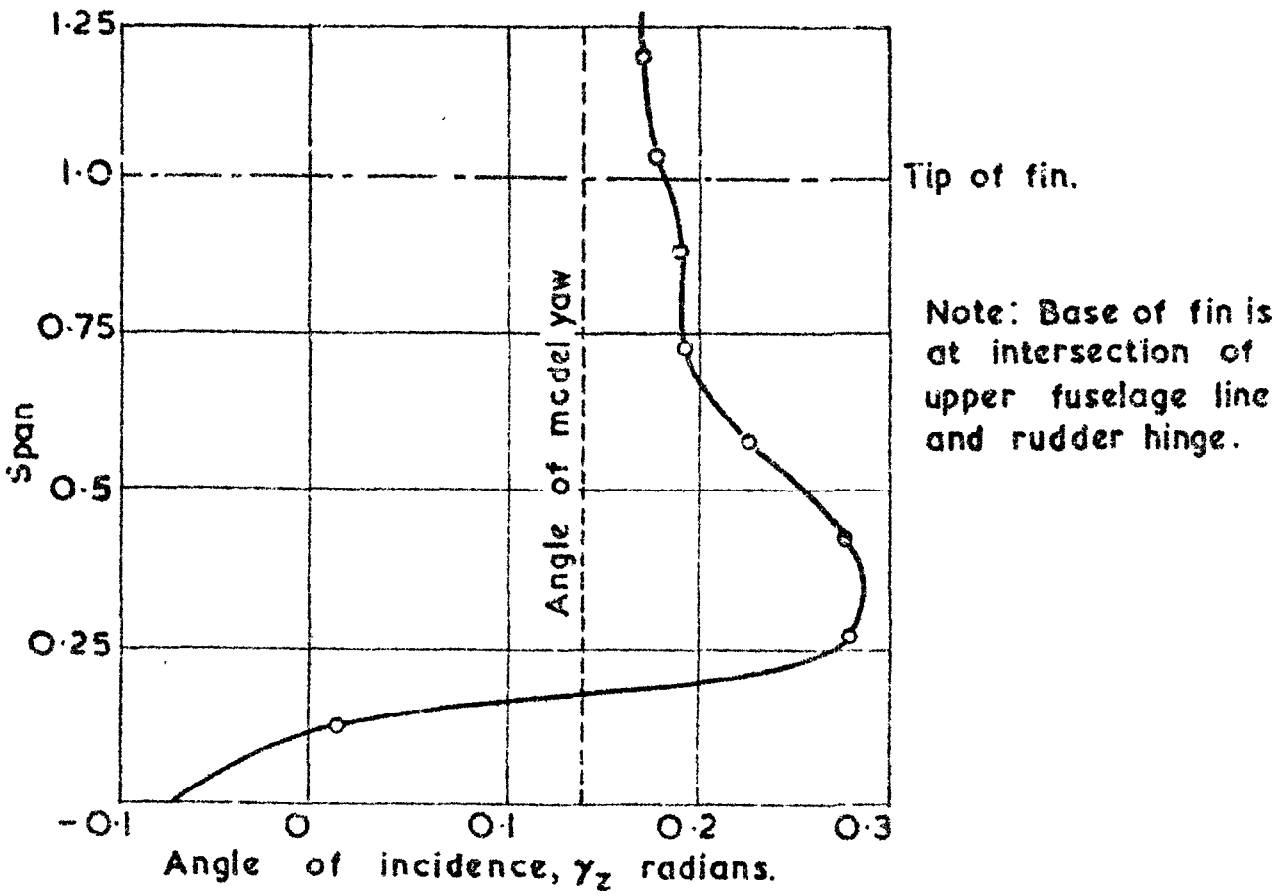

FIG. 7.b.

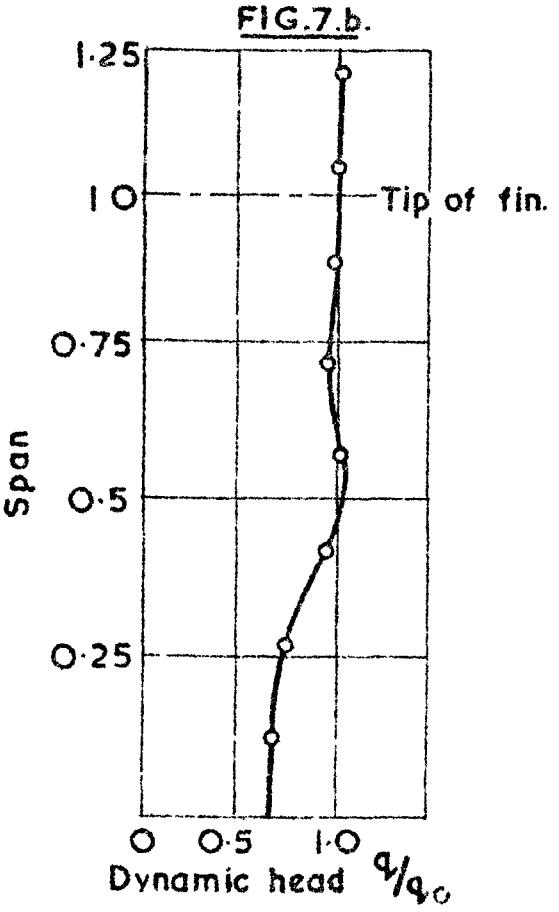

FIG. 7.c

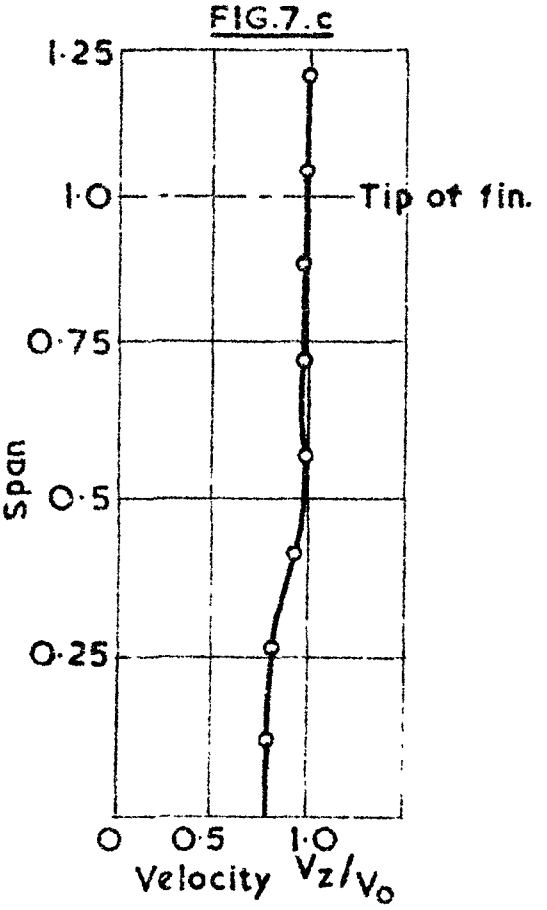

SPANWISE VARIATION OF MEASURED ANGLE OF INCIDENCE, DYNAMIC HEAD AND VELOCITY, LOW TAILPLANE.

FIG. 8. a-c.

FIG. 8a.

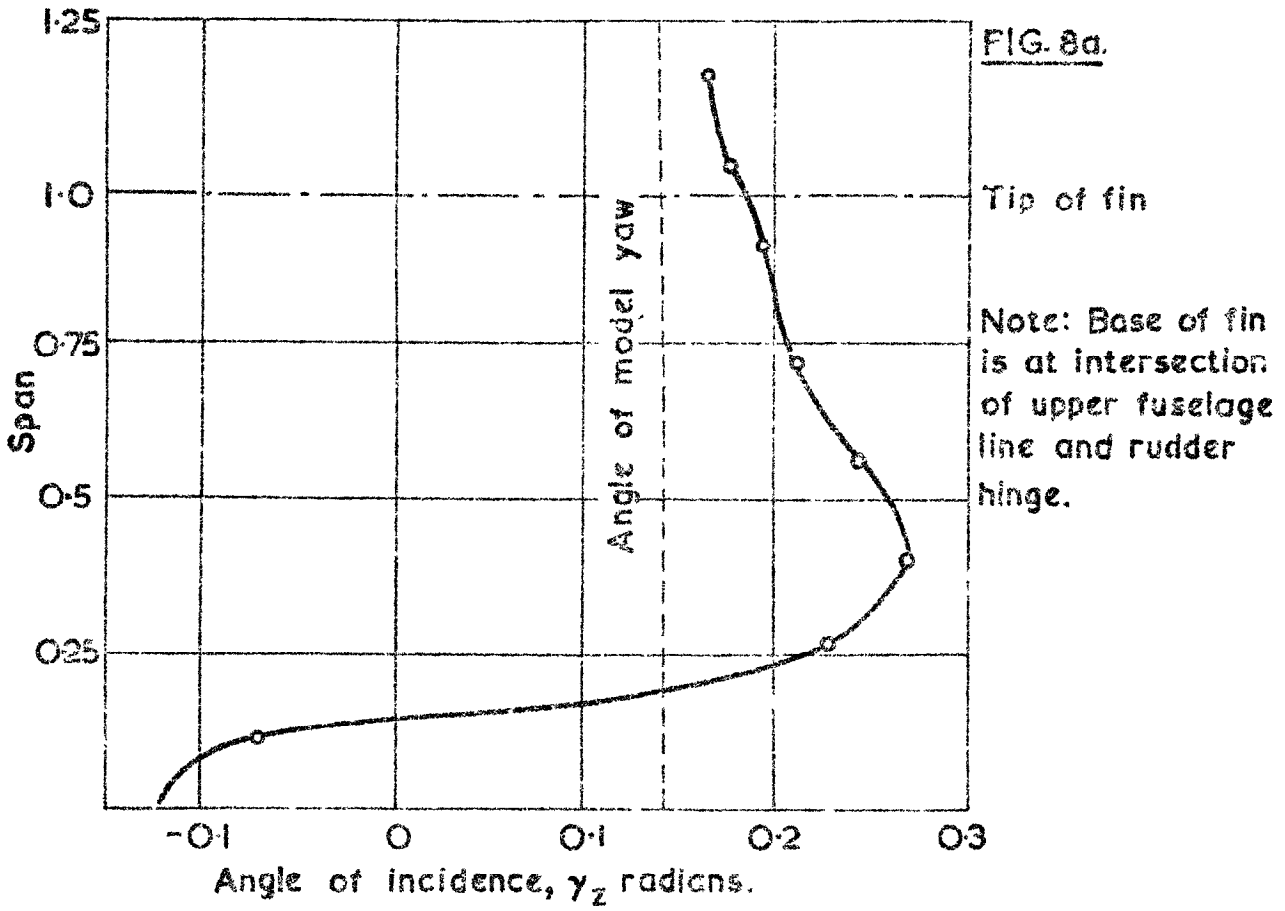

FIG. 8b.

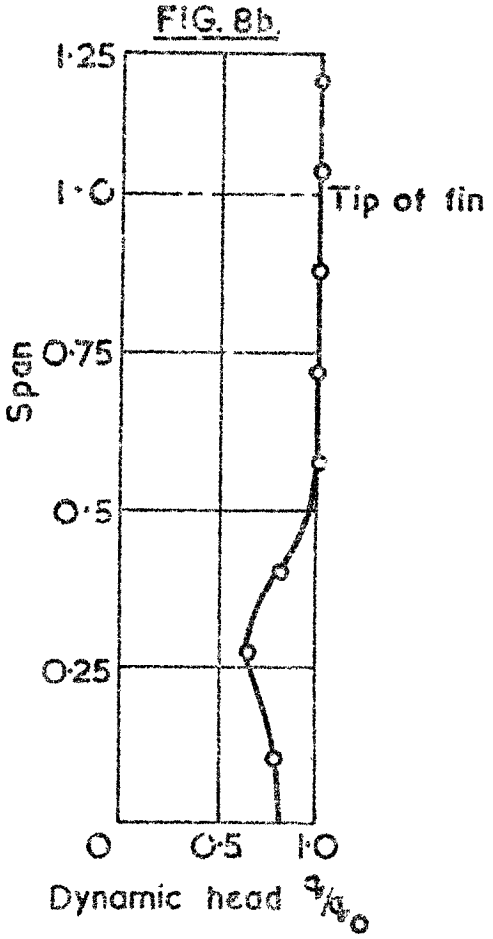

FIG. 8c.

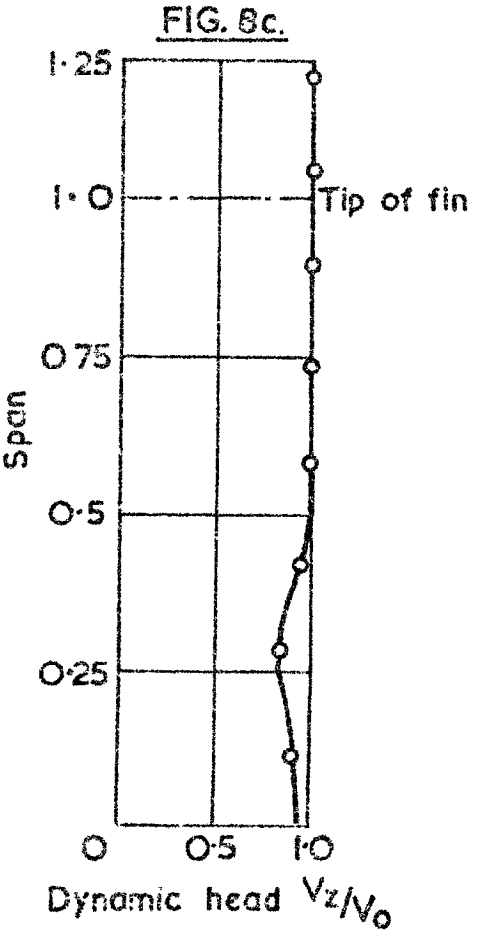

SPANWISE VARIATION OF MEASURED ANGLE OF INCIDENCE, DYNAMIC HEAD AND VELOCITY, HIGH TAILPLANE.

FIG 9

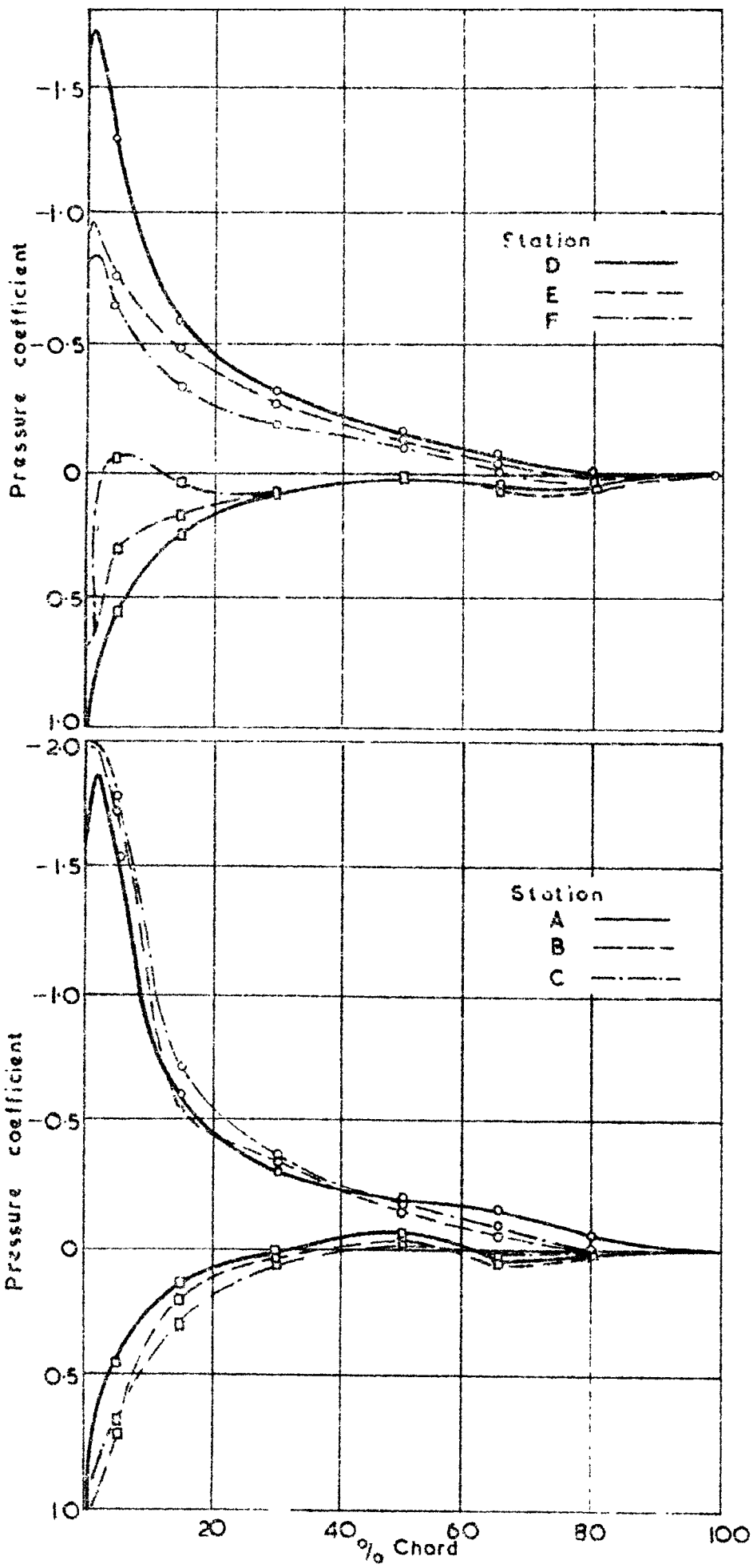

CHORDWISE PRESSURE DISTRIBUTION; LOW TAILPLANE.

FIG.10.

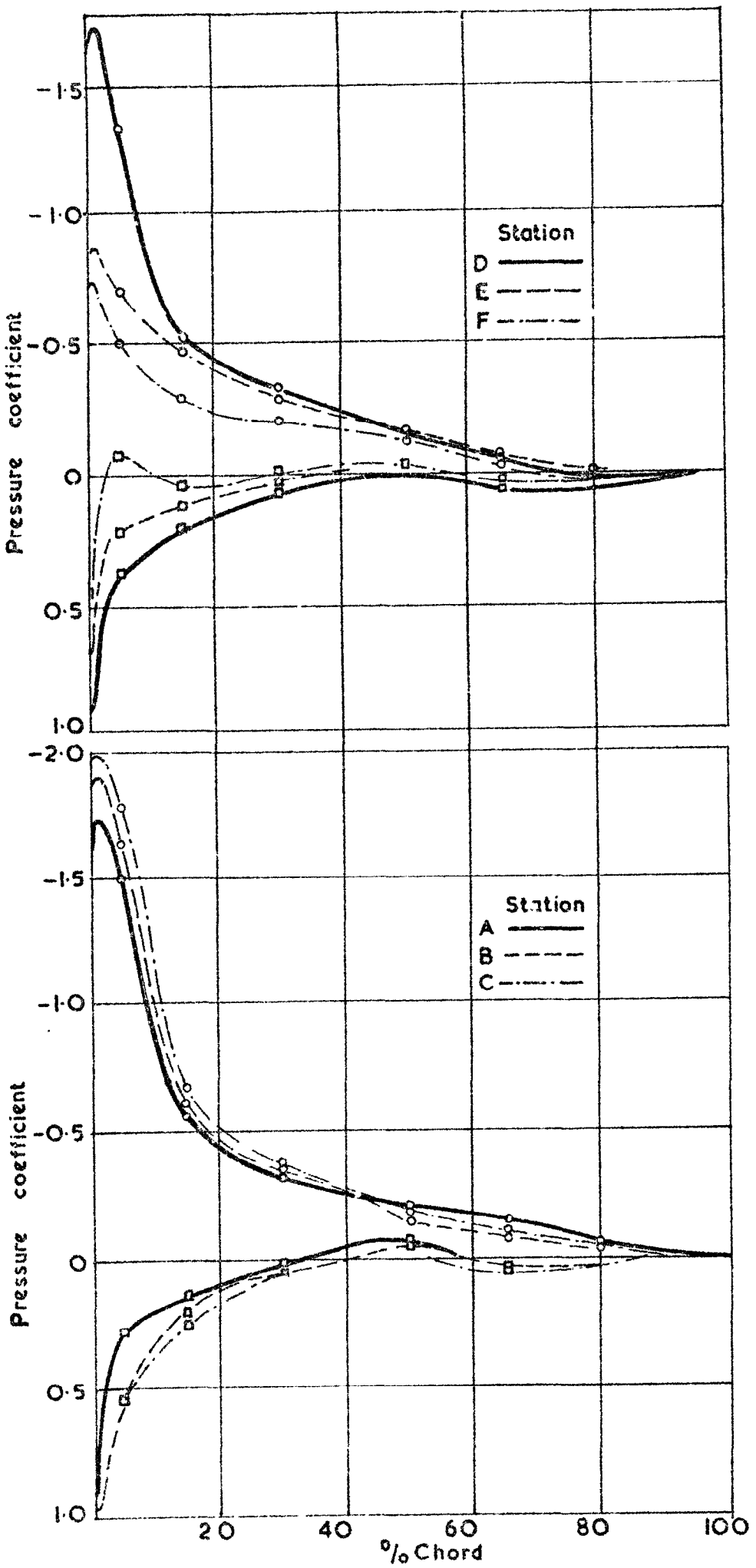

CHORDWISE PRESSURE DISTRIBUTION, HIGH TAILPLANE.

FIG.11.

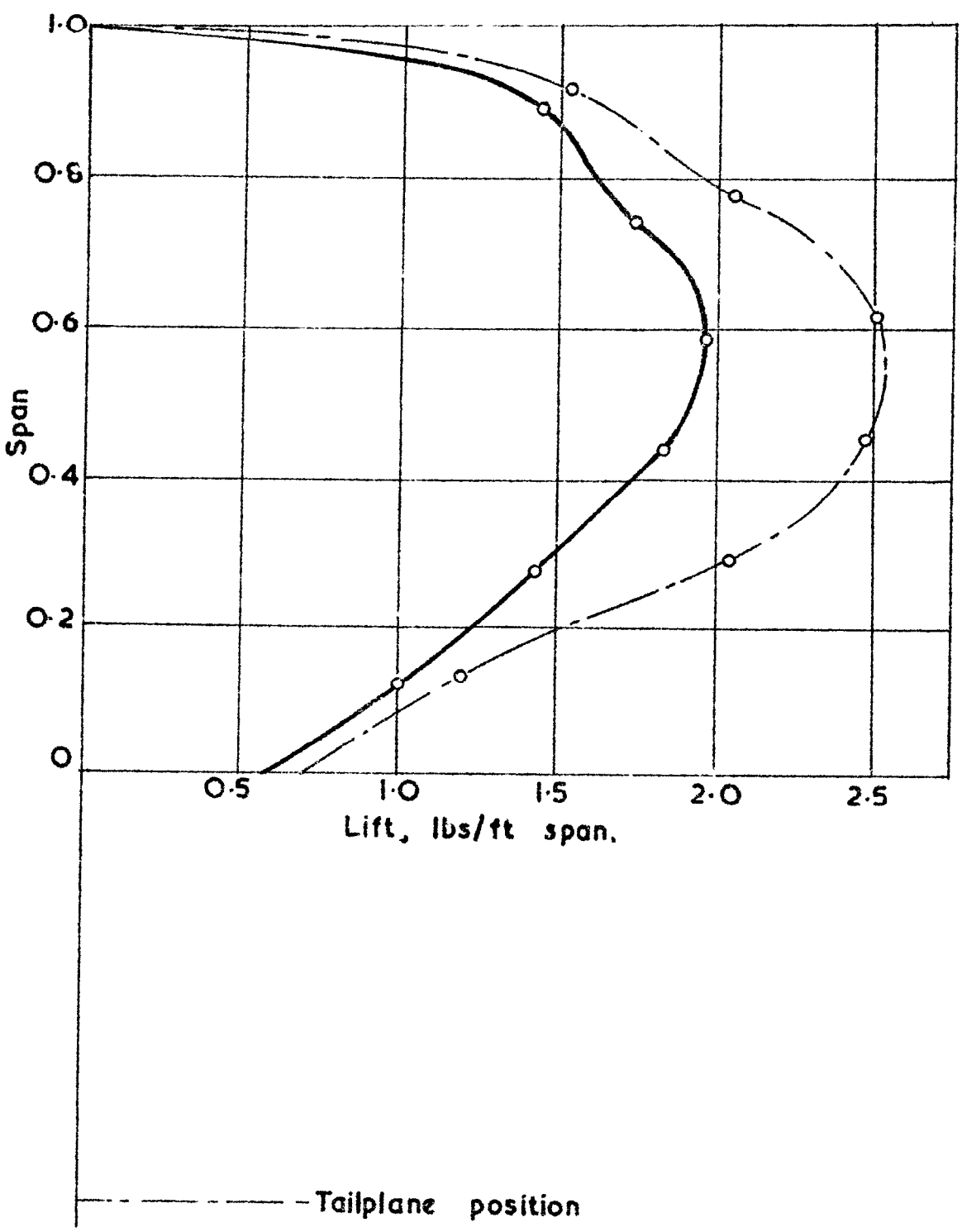

SPANWISE LIFT DISTRIBUTION; LOW TAILPLANE.

FIG. 12.

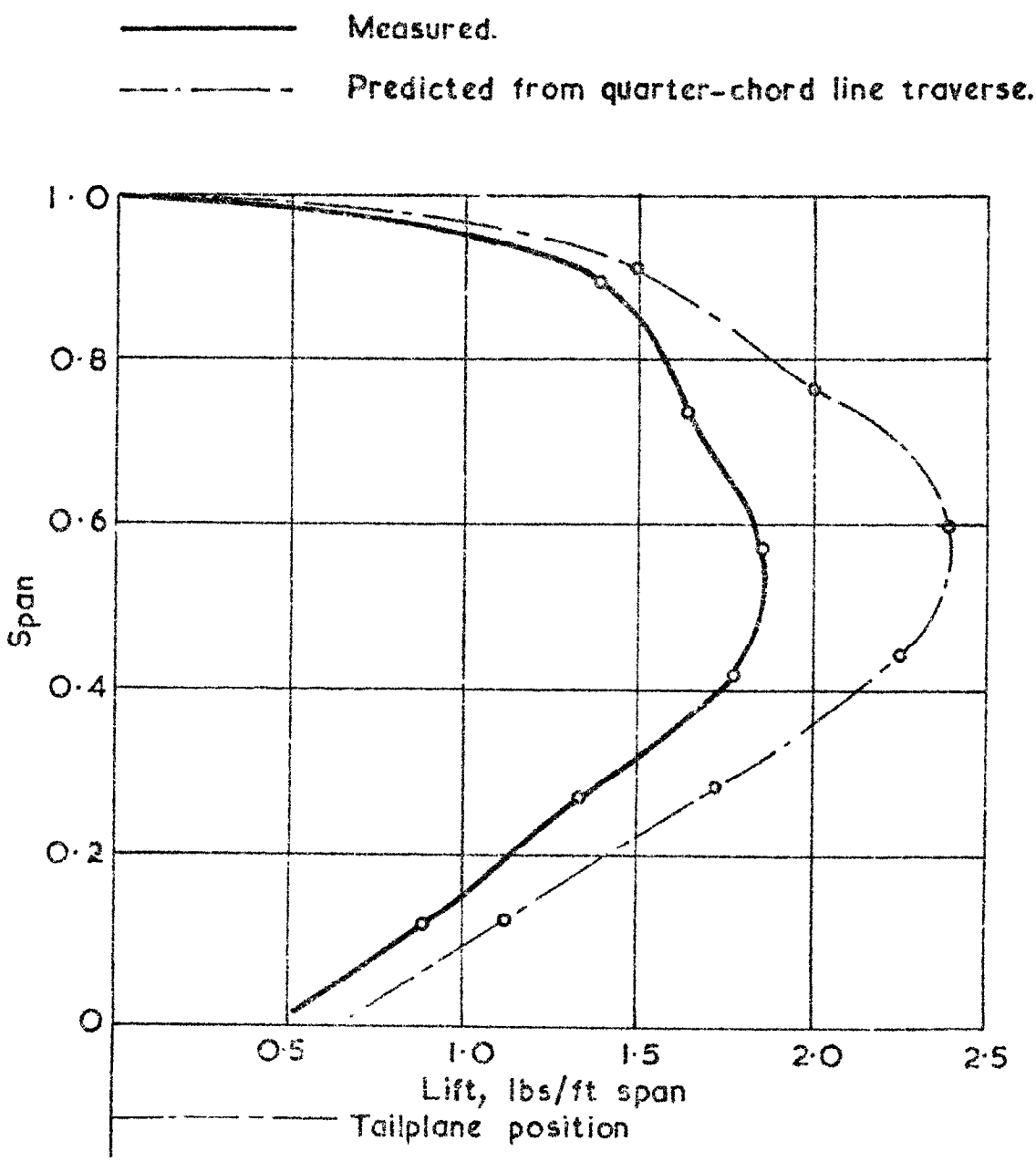

SPANWISE LIFT DISTRIBUTION; HIGH TAILPLANE

FIG. 13.

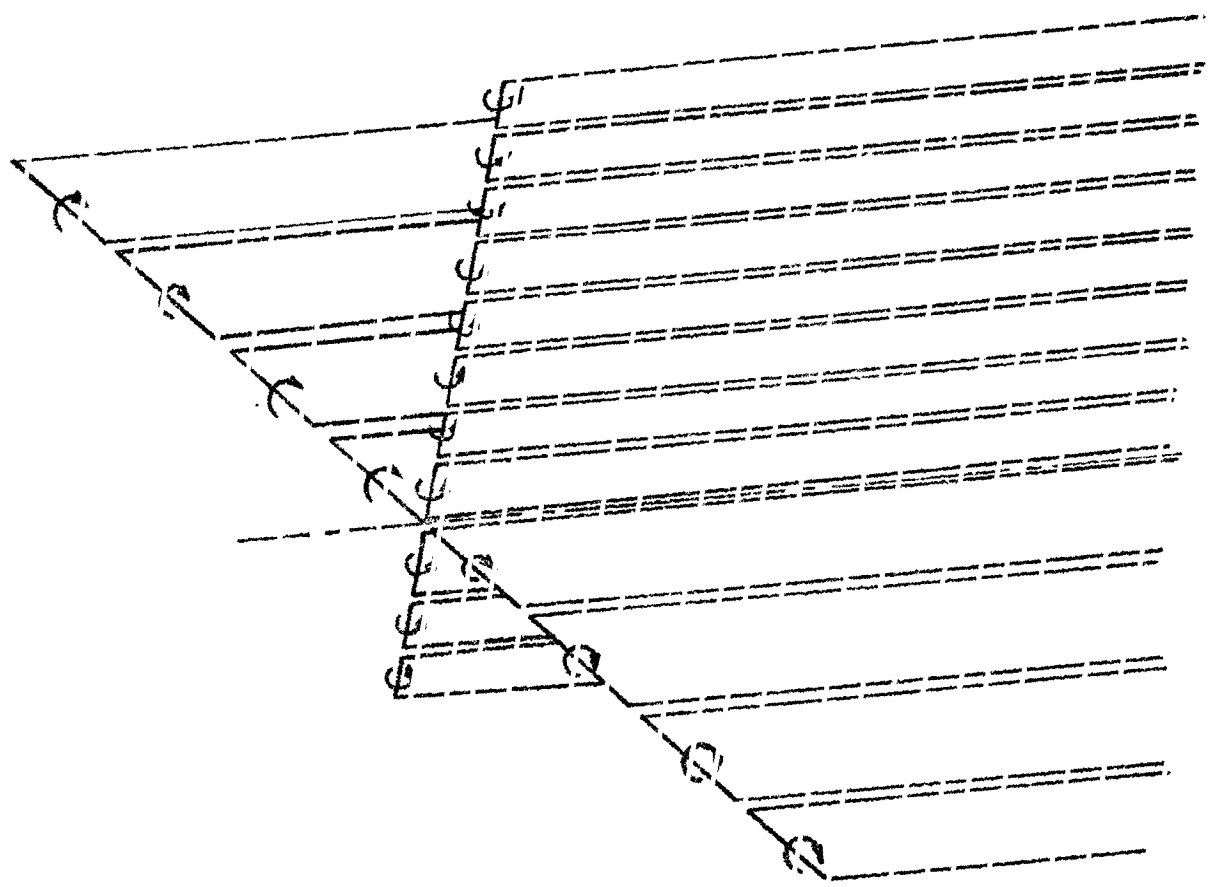

Positive vortices shown

REPRESENTATIVE TAIL UNIT VORTEX SYSTEM

FIG.14.

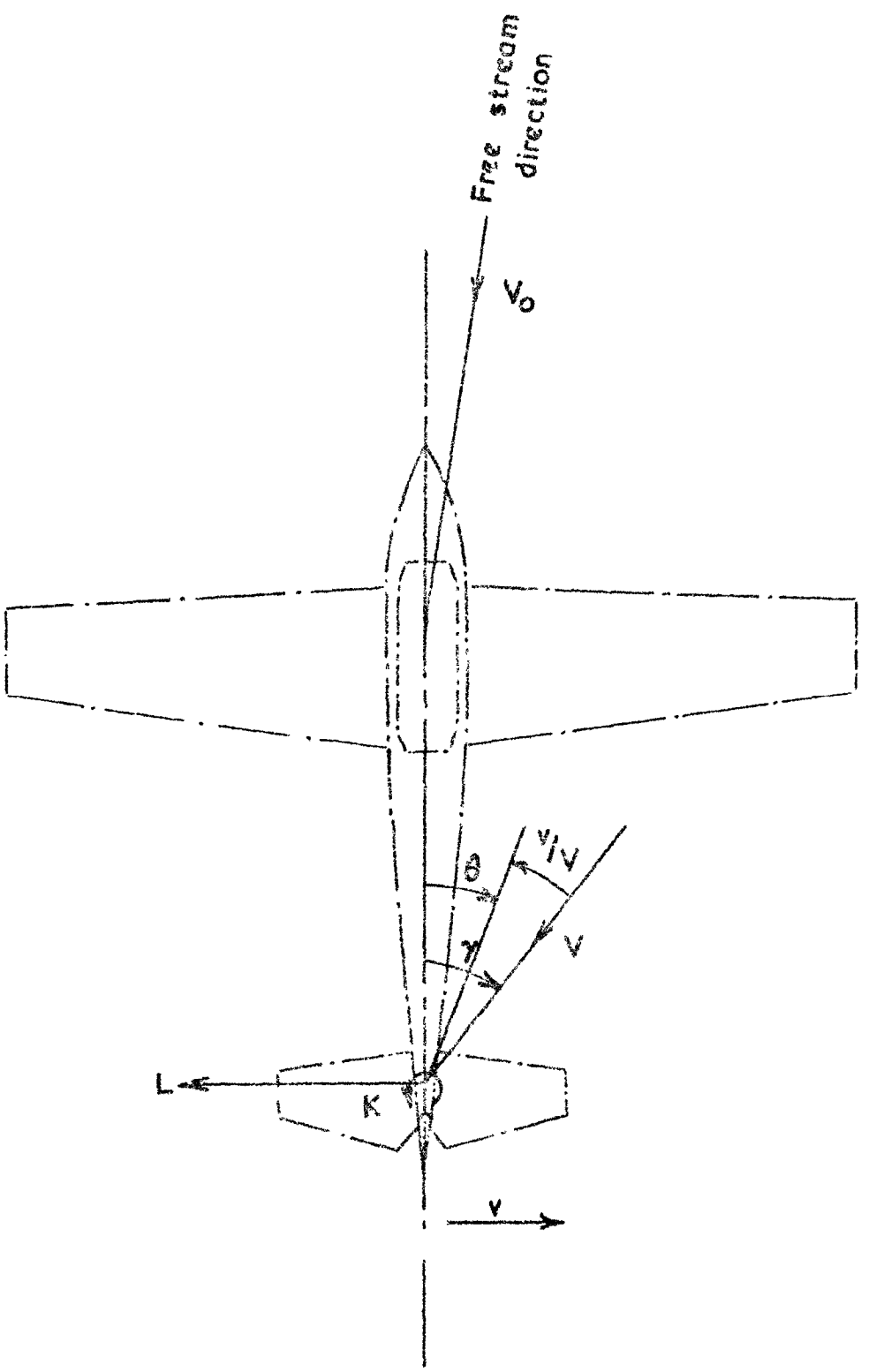

Values shown in positive directions

SIGN CONVENTION.

FIG 15.

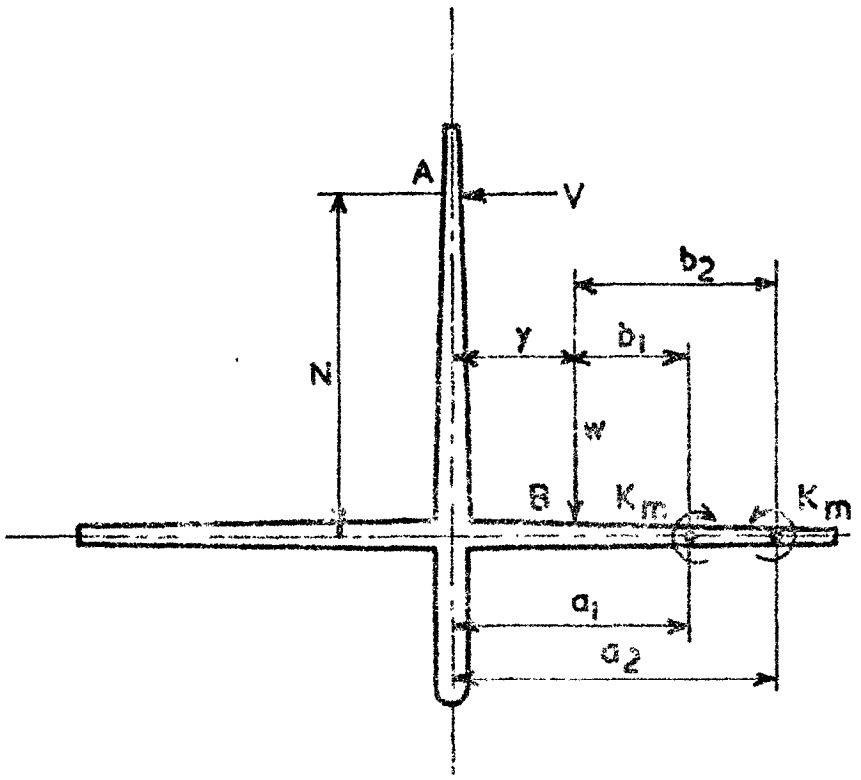

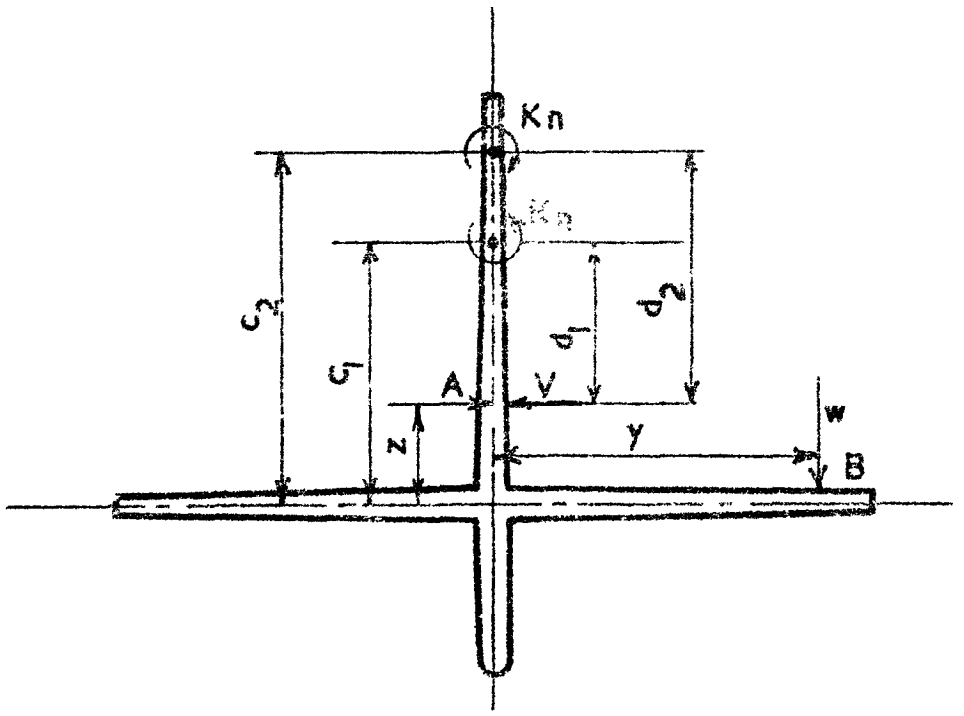

Views looking downstream.

SYMBOLS USED IN VORTEX ANALYSIS.

C.P. No. 491
(19,912)
A.R.C. Technical Report

Printed and published by
HER MAJESTY'S STATIONERY OFFICE

To be purchased from
York House, Kingsway, London w.c.2
423 Oxford Street, London w.1
13A Castle Street, Edinburgh 2
109 St. Mary Street, Cardiff
39 King Street, Manchester 2
Tower Lane, Bristol 1
2 Edmund Street, Birmingham 3
80 Chichester Street, Belfast 1
or through any bookseller

Printed in England

S.O. Code No. 23-9011-91

C.P. No. 491